

DIFFERENCES IN THE SPECTRA OF COSMIC RAY
NUCLEAR SPECIES BELOW ~ 5 GEV/NUC

W. R. Webber, J. A. Lezniak, and J. Kish

Physics Department, University of New Hampshire

Durham, New Hampshire 03824

We have extended previous measurements made at high energies and which show clear evidence for energy dependent changes in cosmic ray composition, to lower energies. This new data points to the fact that these spectral differences extend over the entire energy band from a few hundred MeV/nuc to several 10's of GeV/nuc. The details of these composition variations are examined by studying in a systematic way the variations of the ratios of secondary to primary and different groups of primary cosmic ray nuclei.

1. Introduction. Recently a number of experiments have been performed which reveal differences in the spectra of the cosmic ray nuclear components above several GeV/nuc (Juliusson et al., 1972; Webber et al., 1973; Smith et al., 1973; Ormes and Balasubrahmanyam, 1973). In this paper we report measurements which extend these spectral differences to lower energies and further elucidate these differences in terms of the various nuclear species.

2. Instrumentation and Balloon Flights. This paper reports data obtained on 7 balloon flights in the 1968-72 time period made using two basic detector systems. The lower energy data (200-1500 MeV/nuc) is obtained from a dE/dx x Cerenkov x total energy x range telescope flown at Ft. Churchill in 1970, 1971, and 1972. The 1972 version of this instrument is shown in Figure 1 of paper 043, this conference. For the four flights at a high geomagnetic cut-off rigidity (2.9, 4.1-5.0, and 11.1 GV corresponding to energies from 0.8-4.5 GeV/nuc) we have used a somewhat simplified telescope, replacing the total energy counter with a second Cerenkov detector. This basic telescope has a geometrical factor ~ 600 st cm^2 so that collection factors ~ 2500 events per particle/ m^2 -ster-sec of flux are obtained during a balloon flight. The data format, data analysis procedures, and some details of the charge resolution of this telescope based on the 1970 flight have already been reported (Webber et al., 1972) and will not be discussed here.

3. Derivation of the Energy Spectrum. The fact that up to five separate pulse heights are measured for each particle traversing our telescope allows for a considerable degree of redundancy or consistency to be demanded of these pulse heights. These consistency requirements effectively discriminate against background events - in particular those particles interacting in

the telescope, while at the same time, if applied carefully, will not remove the non-interacting telescope particles. We find the application of consistency criteria to be a much more effective way of removing background events than the use of guard counters. It is also much less susceptible to charge dependent corrections, e.g. knock-on electrons, that are present when guard counters are used, and in addition, the consistency criteria can be varied in a systematic way to study the effects of the criteria on background, etc. In our telescopes the criterion $2 \frac{|S_1 - S_2|}{S_1 + S_2} < 0.3$ is generally applied. For events that satisfy this criterion we construct a series of two dimensional event matrices with axes $\frac{S_1 + S_2}{2}$ vs. C. A sample of such a matrix is shown in Figure 1 for a flight at a geomagnetic cut-off of ~ 2.9 GV. The effects of this cut-off are clearly visible in the Cerenkov distributions for the various nuclei - a similar matrix for a high latitude flight would be populated with events down to the Cerenkov threshold and below.

This Cerenkov distribution is then used to unfold the particle energy spectrum. It is a much more definitive approach than to use the dE/dx dimension for the following reasons: 1) The Cerenkov output is verified to be linear (e.g. the Cerenkov relationship $N = Z^2(1 - E_0^2/E^2)$ holds) to within 2% - as opposed to the well known non-linearities in dE/dx . 2) The Cerenkov distributions for a fixed energy are Gaussian, as opposed to the usual Landau distributions in dE/dx . 3) There is no relativistic rise in the Cerenkov dimension so that the pulse height distribution/relativistic peak may be defined unambiguously in energy and also located more accurately. 4) The relative spread in energy for a given change in pulse height is much greater in the Cerenkov dimension - thus the energies may be located more accurately relative to the peak location than in the dE/dx dimension.

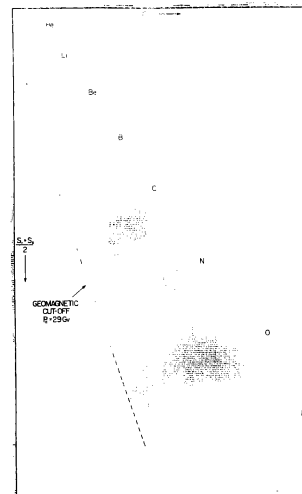


Figure 1. Two dimensional matrix of events $dE/dx \times C$ from balloon flight at cut-off 2.9 GV.

We have written a computer program that convolves the measured Gaussian response functions with the mathematical Cerenkov relationship enabling us to synthesize the Cerenkov pulse height distributions for various input spectra and differential intensities. The differential intensities we quote are based on this analysis as applied identically to the observed Cerenkov distributions for the 1970, 1971, and 1972 high latitude flights.

4. Atmospheric and Instrumental Corrections. The instruments typically float at an atmospheric depth of 3 g/cm^2 which is

roughly equivalent to 0.5 g/cm^2 of interstellar hydrogen in terms of fragmentation. The atmospheric corrections have already been discussed (Webber et al., 1972). The correction for nuclear interactions in the telescope depends on the type of selection criteria imposed. For the selection criteria used in this paper the material in the telescope amounts to between 3 and 4 g/cm^2 for each flight. This introduces a correction which is believed to be well known but is charge dependent and ranges from ~ 1.20 for C nuclei up to ~ 1.60 for Fe nuclei.

5. Results. The differential spectra for various groups of nuclei in the energy range 150-1500 MeV/nuc are shown in Figure 2. The spectra measured in 1970, 1971, and 1972 are shown separately, and it is clear that a large modulation occurred between 1970 and 1971 with a smaller modulation occurring between 1971 and 1972. This is in accord with neutron monitor evidence.

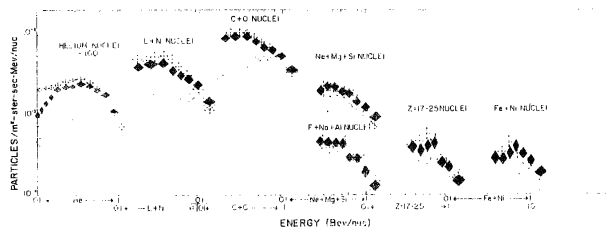


Figure 2. Differential spectra of various groups of nuclei measured in 1970 \diamond , 1971 \blacklozenge , and 1972 \diamond . Symbols remain the same in the following figures.

We show in Table I the integral intensity and intensity ratios for various charge groups obtained on flights at geomagnetic cut-offs of 2.9 and 11.1 GV.

Nuclei	Integral Intensity (particles/m ² -ster-sec)		Ratio $\frac{P_C=2.9}{P_C=11.1}$
	$P_C=2.9 \text{ GV}$	$P_C=11.1 \text{ GV}$	
L+N	3.22 ± 0.05	0.56 ± 0.015	5.72 ± 0.17
C+O	8.15 ± 0.08	1.51 ± 0.03	4.51 ± 0.08
Ne+Mg+Si	1.80 ± 0.04	0.40 ± 0.013	4.28 ± 0.15
F+Na+Al	0.38 ± 0.02	0.06 ± 0.005	6.07 ± 0.56
Z=17-25	0.39 ± 0.02	0.048 ± 0.005	7.55 ± 0.74
Fe+Ni	0.32 ± 0.016	0.13 ± 0.010	2.52 ± 0.18

From the data in Figure 2 and Table I as well as earlier data from a telescope employing a gas Cerenkov detector (Webber et al., 1973) we may construct a series of ratios of the intensity of various groups of nuclei as a function of energy. Some of these ratios are shown in Figures 3, 4, 5, 6, and 7. There is a reason for dividing up the nuclei into these particular charge groups. He, C+O, Ne+Mg+Si, and Fe+Ni represent groups of nuclei that are mainly primary or source nuclei. Li+Be+B=L+N, F+Na+Al and Z=17-25 are mainly secondary or fragmentation nuclei.

Consider first the ratios of groups of primary nuclei, e.g. He/C+O, C+O/Fe+Ni and He/Fe+Ni. All of these ratios are ob-

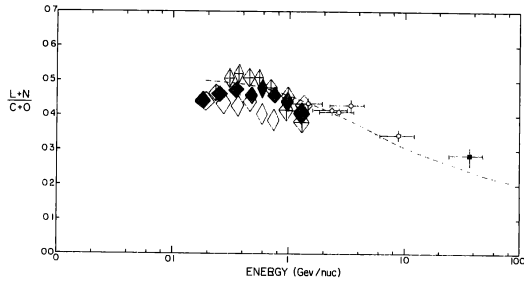


Figure 3. Ratio of L+N to C+O nuclei. Integral measurements using earth's magnetic field \circ and above the gas Cerenkov threshold \blacksquare are shown as differential points at twice the threshold energy.

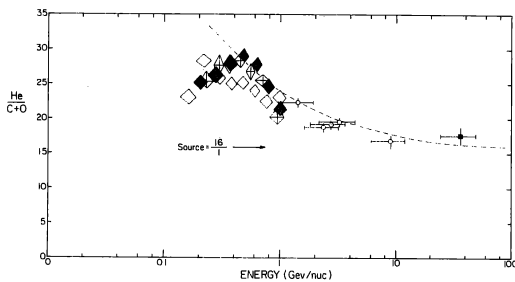


Figure 5. Ratio of He to C+O nuclei.

served to vary with energy at high energies as has already been observed, but at low energies as well, at least down to a few hundred MeV/nuc. The same behavior is observed for the ratio of a group of secondary nuclei to a group of primary nuclei, e.g. L+N/C+O, Z=17-25/Fe+Ni. Thus the energy dependent charge ratios are not confined to high energies as was previously believed.

The charge ratios observed at low energies are pretty much the same in years 1970-71-72, however, there is some evidence of a systematic trend for slightly higher ratios in 1971 and 1972. This is to be expected from solar modulation as will be discussed later.

6. Interpretation of Results. In this short article we cannot

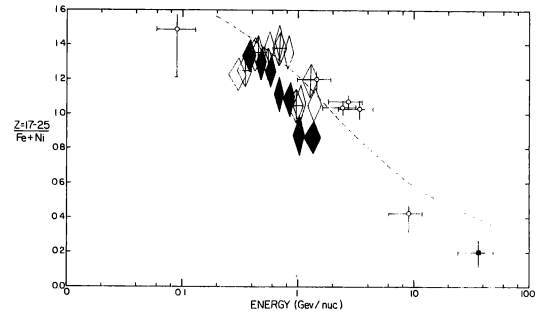


Figure 4. Ratio of Z=17-25 to Fe+Ni nuclei.

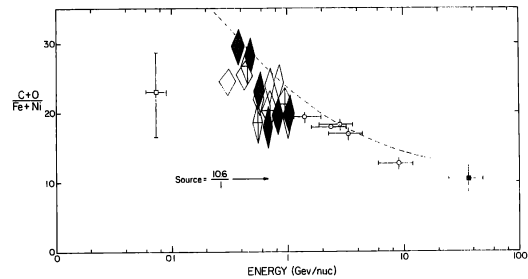


Figure 6. Ratio of C+O to Fe+Ni nuclei.

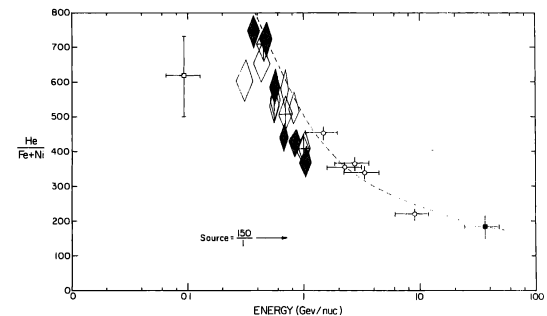


Figure 7. Ratio of He to Fe+Ni nuclei.

obviously discuss these energy dependent variations in great detail. We will be satisfied with a brief summary of the relevant data and some of the more obvious theoretical implications. First we observe that the intensity ratios of secondary to primary nuclei increase at lower energies indicating that the secondary nuclei have steeper spectra. Second, we find that the ratio of two primary nuclei also increases at lower energies if we take the ratio of the lightest nuclei to the heaviest, again implying steeper spectra for the lighter nuclei. This is a systematic effect and is observed for Ne+Mg+Si nuclei as well and is not only related to an anomalous Fe+Ni spectrum.

Previously we (Webber et al., 1973) have interpreted both these types of effects in terms of an energy dependent path length for cosmic ray matter traversal in the galaxy in which lower energy particles have longer matter lengths in g/cm^2 . This is a very obvious conclusion to be drawn from the decreasing secondary to primary ratios at high energies since if the fragmentation cross sections are relatively constant with energy as one believes, the only way to obtain a smaller abundance of secondary nuclei at high energies is to pass them through less matter. We also pointed out that an energy dependent path length will effect the ratios of groups of primary nuclei as well. In the exponential path length distribution model for cosmic ray propagation in the galaxy a term $[\frac{1}{\lambda_i} + \frac{1}{\lambda_e}]^{-1}$ occurs (λ_i =interaction MFP, λ_e =escape MFP in g/cm^2). This term is sort of an "equivalent" path length in this model and because of the different values for λ_i of the source nuclei, a λ_e that changes with energy will also produce surprisingly large variations in the ratios of different source nuclei.

We have refined our earlier treatment for the cosmic ray propagation which was applicable at high energies and have written a computer program which, using the steady state exponential path length model, considers the fragmentation of each nucleus and its variation with energy according to the best known data, as well as energy loss by ionization. We determine the spectrum of each nucleus or charge group and the corresponding charge ratios for various assumptions regarding $\lambda_e(E)$ - assuming that initially each nucleus has the same total energy spectrum. The calculated spectra and charge ratios refer to those incident on the solar system. We have made no attempt to account for solar modulation at this stage of the calculations. The dashed curves in Figures 3-7 represent the variations predicted at the boundary of the solar system if $\lambda_e \sim 5 (\frac{E_0}{E})^{1/2} g/cm^2$, $E_0 = 5$ GeV/nuc, and the source ratios are as indicated on the figures. The agreement between the predictions and measurements is striking indeed.

If solar modulation effects result in an effective energy loss of several hundred MeV/nuc for low energy nuclei then the observed ratios at earth should lie progressively to the left of the dashed curve at lower energies - indeed the observed ratios

1973ICRC.....1..248W

at earth should be almost flat at the lowest energies. An increase in the ratios at lower energies should also be noticed between 1970 and 1972 because of the greatly decreased modulation. Given precise enough data, this behavior could be used to determine the total energy loss in interplanetary space resulting from solar modulation and to determine the local interstellar spectra and charge ratios in an independent manner. The actual data shows clear evidence of the trends expected, although systematic uncertainties in the year to year results make these tests less definitive.

We close by noting that we have only argued that the data strongly indicate a cosmic ray path length in the galaxy varying continuously with energy throughout the range from a few hundred MeV/nuc to many GeV/nuc. We have not discussed the further implications of this apparent energy dependence in terms of cosmic ray propagation, source distribution and source effects - but needless to say the implications in these directions are profound.

Acknowledgments. This work was performed under NASA grant NGR 30-002-052.

References

Juliusson, E., Meyer, P., and Muller, D., Phys. Rev. Lett., 29, 445, 1972.

Ormes, J. F. and Balasubrahmanyam, V. K., Nature Phys. Sci., 241, 95, 1973.

Smith, L. H., Buffington, A., Smoot, G. F., and Alvarez, L. W., Astrophys. J., 180, 987, 1973.

Webber, W. R., Lezniak, J. A., Kish, J. C., and Damle, S. V., Nature Phys. Sci., 241, 96, 1973.

Webber, W. R., Damle, S. V., and Kish, J., Astrophys. and Space Sci., 15, 245, 1972.